https://doi.org/10.5194/bg-2022-246
Preprint. Discussion started: 4 January 2023

Biogeosciences Discussions
Open Access
EGU

Seasonal cycles of biogeochemical fluxes in the Scotia Sea, Southern Ocean: A stable isotope approach

Anna Belcher[1], Sian F. Henley[2], Katharine Hendry[1,3], Marianne Wootton[4], Lisa Friberg[3], Ursula Dallman[2], Tong Wang[3], Clara Manno[1]

[1] British Antarctic Survey, Cambridge, CB3 0ET, UK

[2] School of Geosciences, University of Edinburgh, Edinburgh EH9 3FE, UK

[3] University of Bristol, Bristol, BS8 1RJ, UK

[4] Marine Biological Association, Plymouth, PL1 2PB, UK

Correspondence to: Anna Belcher (annbel@bas.ac.uk) and Clara Manno (clanno@bas.ac.uk)

Abstract

The biological carbon pump is responsible for much of the decadal variability in the ocean carbon dioxide (CO_2) sink, driving the transfer of carbon from the atmosphere to the deep ocean. A mechanistic understanding of the ecological drivers of particulate organic carbon (POC) flux is key to both the assessment of the magnitude of the ocean CO_2 sink, as well as for accurate predictions as to how this will change with changing climate. This is particularly important in the Southern Ocean, a key region for the uptake of CO_2 and the supply of nutrients to the global thermocline. In this study we examine sediment trap derived particle fluxes and stable isotope signatures of carbon (C), nitrogen (N) and biogenic silica (BSi) at a study site in the biologically productive waters of the northern Scotia Sea in the Southern Ocean. Both deep (2000 m) and shallow (400 m) sediment traps exhibited two main peaks in POC, particulate nitrogen and BSi flux, one in austral spring and one in summer, reflecting periods of high surface productivity. Particulate fluxes and isotopic compositions were similar in both deep and shallow sediment traps, highlighting that most remineralisation occurred in the upper 400 m of the water column. Differences in the seasonal cycles of isotopic compositions of C, N and Si provide insights into the degree of coupling of these key nutrients. We measured increasing isotopic enrichment of POC and BSi in spring, consistent with fractionation during biological uptake. Since we observed isotopically light particulate material in the traps in summer, we suggest physically-mediated replenishment of lighter isotopes of key nutrients, enabling full expression of the isotopic fractionation associated with biological uptake. The change in the nutrient and remineralisation regimes, indicated by the different isotopic baselines of the spring and summer productive periods suggests to a change in the source region of material reaching the traps, and associated shifts in phytoplankton community structure. This, combined with the occurrence of advective inputs at certain times of the year, highlights the need to make synchronous measurements of physical processes to be able to better track changes in the source regions of sinking particulate material. We also highlight the need to conduct particle specific (e.g. faecal pellet, phytoplankton detritus, zooplankton moults) isotopic analysis to improve the use of this tool in

https://doi.org/10.5194/bg-2022-246
Preprint. Discussion started: 4 January 2023

assessing particle composition of sinking particulate material and develop our understanding of the drivers of biogeochemical fluxes.

1. Introduction

The transfer of carbon from the atmosphere to the deep ocean via the biological carbon pump (BCP, Volk and Hoffert, 1985) is important for the sequestration of carbon, and combined with ocean circulation is a main driver of decadal variability of the ocean carbon dioxide (CO_2) sink (DeVries, 2022). Mechanistic understanding of the processes controlling the magnitude and efficiency of the BCP is therefore key to assessment and prediction of the ocean's role as a CO_2 sink and requires robust characterisation of the composition of the sinking particles transferring particulate organic carbon (POC) to the deep ocean.

Sediment traps enable visual assessment of sinking particles, and have been deployed in numerous locations throughout the world's oceans to both quantify biogeochemical fluxes and characterise the nature of sinking material (for example data compilation of Atlantic Ocean sediment traps; Torres Valdés et al., 2014). Numerous studies have recorded the dominance of particular organisms or types of detrital material, highlighting the importance of ecosystem community structure on the magnitude and efficiency of the BCP. For example, faecal pellets, diatoms, diatom resting spores and acantharia have been observed as significant contributors to particle fluxes (González et al., 2009; Belcher et al., 2018, 2017; Manno et al., 2015; Gleiber et al., 2012; Rembauville et al., 2015; Roca-Marti et al., 2017). Such visual assessment of trap material is typically very time consuming. Additionally, fragile material, such as salp faecal pellets (Iversen et al., 2017; Pauli et al., 2021) may break up in the sample manipulation processes, making them hard to account for visually. Biogeochemical methods such as the use of stable isotopes may offer additional insight into the drivers of POC fluxes (e.g. Henley et al., 2012).

Marine phytoplankton take up aqueous CO_2 ($[CO_{2(aq)}]$) during photosynthesis, converting it to organic carbon. During this process, the lighter isotope (^{12}C) is preferentially assimilated, which enriches the residual aqueous pool in the heavier isotope (^{13}C). The stable isotopic composition of the POC ($\delta^{13}C_{POC}$) of the marine phytoplankton is therefore lower than the carbon source. Over large scales, the $\delta^{13}C$ of marine phytoplankton has been found to be inversely correlated with $[CO_{2(aq)}]$ in surface waters (Rau et al., 1991). However, numerous other factors have been identified as impacting the $\delta^{13}C_{POC}$ of surface waters and marine plankton. Phytoplankton growth rates, cell geometry and non-diffusive uptake of carbon via carbon concentration mechanisms have all been highlighted as impacting the $\delta^{13}C_{POC}$ of marine plankton and thus surface waters (Popp et al., 1999, 1998; Bidigare et al., 1999; Trull and Armand, 2001; Tuerena et al., 2019). This decoupling of the relationship between $\delta^{13}C_{POC}$ and $[CO_{2(aq)}]$ presents complications for palaeoceanographic studies, but presents the possibility of using the $\delta^{13}C_{POC}$ of marine samples to infer information about community composition.

During photosynthetic uptake, the balance between supply and demand of carbon impacts $\delta^{13}C_{POC}$, regulated by the transport into the internal cell and fixation to organic carbon (Popp et al., 1999; Trull and Armand, 2001). A greater isotopic fractionation occurs in smaller phytoplankton cells, enabled by the higher cell surface area to volume (SA:V) ratios and increased amount of $[CO_{2(aq)}]$ diffusing across the cell membrane relative to the total carbon within the cell (Popp et al., 1998;

https://doi.org/10.5194/bg-2022-246
Preprint. Discussion started: 4 January 2023

Tuerena et al., 2019; Hansman and Sessions, 2016). Thus, a community dominated by large, fast-growing diatoms is expected to contribute to enriched $\delta^{13}C_{POC}$ values compared to a community dominated by picoplankton. A study by Henley et al. (2012) in the coastal western Antarctic Peninsula, attributed a large (~10‰) negative isotopic shift in $\delta^{13}C_{POC}$ to a near-complete biomass dominance of the marine diatom *Proboscia inermis* highlighting the possible impact of shifts in species composition on stable isotopes. It may therefore be possible to use stable isotopes to gain information about the community composition of phytoplankton driving, for example, large spring pulses in POC flux. Additionally, siliceous phytoplankton, such as diatoms, require dissolved silica (silicic acid, or DSi) to build their cell walls or frustules (amorphous SiO_2 nH_2O, referred to here as biogenic silica, BSi), and isotopic fractionation occurs during cell wall formation (De La Rocha et al., 1997). This means that BSi fluxes and ratios of light ^{28}Si to heavy ^{30}Si (expressed as $\delta^{30}Si$) in sinking particulate organic matter (POM) can be informative about DSi utilisation by siliceous phytoplankton.

Additionally, the stable isotopes of marine nitrogen reveal information about uptake of inorganic nitrogen sources by phytoplankton (Wada and Hattori, 1978), as well as trophic and food web processes (Michener and Lajtha, 2008). Different sources of nitrogen can alter the baseline stable isotopic composition ($\delta^{15}N$) of marine phytoplankton because ammonium characteristically has a lower value of $\delta^{15}N$ than nitrate supplied from depth. As well as this, isotopic fractionation occurs during transfer through the food-web, with a trophic enrichment of typically 2- 4‰ between successive trophic levels (Montoya, 2007; Minagawa and Wada, 1984). Excretion and egestion processes can impact $\delta^{15}N$; isotopic discrimination during excretion of ammonium by zooplankton and fish results in ammonium that is ^{15}N-depleted relative to the substrate (Montoya, 2007). Thus, there are several interacting processes impacting the degree of fractionation and subsequent isotopic ratios in particulate nitrogen (PN) and knowledge of $\delta^{15}N$ ratios may provide insight into biogeochemical processes and the composition of the sinking flux.

In this study we examine the seasonal cycle, magnitude and composition of vertical biogeochemical fluxes of particulate material collected by two sediment traps deployed for a year on a deep ocean mooring located in the northern Scotia Sea (Atlantic sector of the Southern Ocean). The Scotia Sea, particularly the region downstream of South Georgia is a hot spot for biological productivity, supported by higher iron availability (Korb et al., 2008; Matano et al., 2020). Diatoms dominate the phytoplankton assemblage, particularly in the summer months, with smaller contributions of dinoflagellates (Korb et al., 2012). The large, consistent phytoplankton blooms occurring in this region support high fluxes of POC to the deep ocean, with two peaks in POC occurring during the seasonal cycle (first peak in austral spring, and second in late summer or early autumn) (Manno et al., 2015). Faecal pellets (up to 91% seasonally (Manno et al., 2015)), krill exuviae (up to 47% seasonally (Manno et al., 2020)) and diatoms, particularly resting spores (42% annually (Rembauville et al., 2016)) have been shown to make a large contributions to the POC fluxes in our study region. Here we use $\delta^{13}C_{POC}$, $\delta^{15}N_{PN}$ and $\delta^{30}Si_{BSi}$ as tools to reveal information on the composition of organic matter and processes influencing its production and subsequent flux to depth. More in-depth understanding of the composition, and thus the drivers of POC flux in this important region are key to improving estimates of the current and future strength of the BCP and the ocean's role as a CO_2 sink.

https://doi.org/10.5194/bg-2022-246
Preprint. Discussion started: 4 January 2023

2. Methods

2.1. Study Area

This study was conducted in the open ocean environment of the northern Scotia Sea in the Southern Ocean at a long-term observatory station, P3 (Figure 1), where an oceanographic mooring is located. The mooring is part of the Scotia Sea Open Ocean Observatory (SCOOBIES: https://www.bas.ac.uk/project/scoobies/), a programme designed to investigate the biological and biogeochemical influence of the large and persistent phytoplankton bloom to the northwest of South Georgia.

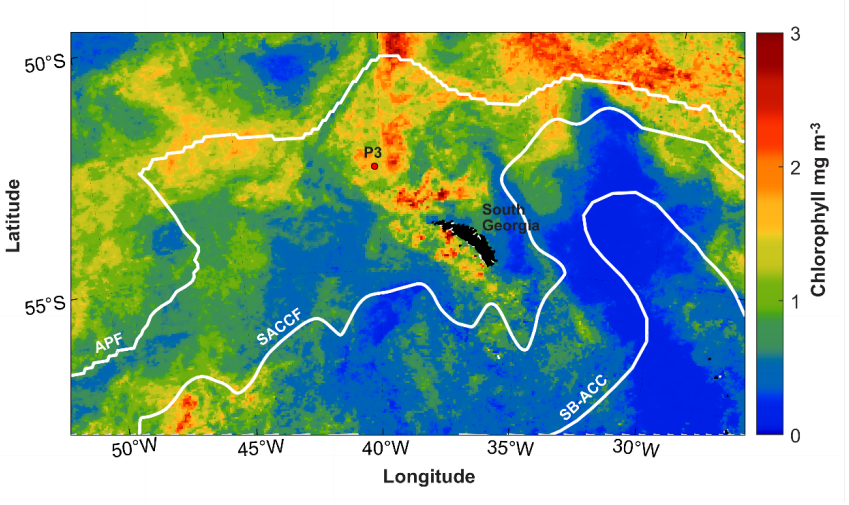

Figure 1: Location of P3 mooring site to the northwest of South Georgia. White lines indicate frontal positions of the Antarctic Polar Front (APF) **(Moore et al., 1999)*, Subantarctic Circumpolar Current Front (SACCF)*** **(Thorpe et al., 2002)** ***and the Southern Boundary of the Antarctic Circumpolar Current (SB-ACC)*** **(Orsi et al., 1995)*. Mean chlorophyll concentration (mg m^{-3}) is shown for December 2018 from 8 day satellite chlorophyll data from the Ocean Colour CCI (version 5.0)*** **(Sathyendranath et al., 2021, 2019).**

2.2. Sediment trap deployment

Two sediment traps were deployed on the mooring array to collect sinking particles for analysis of carbon, nitrogen and biogenic silica fluxes and analysis of $\delta^{13}C_{POC}$, $\delta^{15}N_{PN}$ and $\delta^{30}Si_{BSi}$. The mooring was deployed from January 2018, during research cruise JR17002 aboard the *RRS James Clark Ross,* to January 2019, recovered during research cruise DY098 aboard the *RRS Discovery.* The mooring was located at -52.8036 °N, -40.1593 °E, to the northwest of South Georgia island in the Scotia Sea at a water depth of 3748 m. Sediment traps (McLane PARFLUX, 0.5 m^2 surface collecting area; McLane labs, Falmouth, MA, USA) were deployed at 400 and 2000 m (referred herein as shallow and deep respectively) and were each equipped with 21 sample bottles. A baffle at the top of the trap prevents large organisms from entering and each bottle contained a formosaline solution (filtered seawater containing 2% v/v formalin, mixed with sodium tetraborate (BORAX; 0.025% w/v), and 0.5% w/v sodium chloride) to prevent mixing with the overlying water column and stop biological

https://doi.org/10.5194/bg-2022-246
Preprint. Discussion started: 4 January 2023

degradation. Previous studies have reported the effects of formalin on $\delta^{13}C$ and $\delta^{15}N_{PN}$ to be small (±1‰ and ±1.5‰ respectively) (Mincks et al., 2008 and refs. within), which are small compared to the isotopic shifts we observed. Yet we stress that all given values are associated with this uncertainty. The sediment trap sample carrousel was programmed to rotate every 7-31 days depending on the season; shorter periods to coincide with austral summer and longer periods during austral winter (Table S1). Seaguard current meters were deployed ~50m above/below the shallow/deep sediment traps respectively, set at a measurement interval of 2 hours.

2.3. Trap sample processing

Each sample from the sediment trap was processed on return to the laboratory. The supernatant was carefully removed using a syringe and swimmers (zooplankton that are believed to have entered the trap actively whilst alive) were removed. Swimmers were removed by hand under a dissecting microscope and were not included in flux calculations. Each sample was split into a number of smaller aliquots for subsequent analysis using a McLane rotary splitter.

2.3.1.Organic carbon and nitrogen

For each sediment trap sample (from both deep and shallow traps), two or three splits were analysed for POC and PN. Once split, the material was filtered onto pre-combusted (450 °C, 24h) 25 mm glass fibre filters (GF/F) and rinsed with milli-Q water. Samples were air dried before fuming for 24 h with 37% HCl in a desiccator, before finally oven-drying at 50 °C for 24 h. Filters and filter blanks were placed in pre-combusted (450 °C, 24 h) tin capsules (Hilton et al., 1986), and POC and PN measured on a CE Instruments NA2500 Elemental analyser, calibrated using an acetanilide calibration standard with a known %C and N of 71.09% and 10.36% respectively. Standards were interspersed regularly between samples to correct for drift. Analytical precision was better than 1.0% for POC and 1.1% for PN. The POC flux (*F*) for each sample was calculated using the following equation:

$$F(mg\ C\ m^{-2}d^{-1}) = m/(A \times d) \quad (1)$$

Here *m* is the mass of POC in the sample bottle (mg), *d* is the number of days that the sample bottle was open (7–31 days) and *A* is the surface area of the sediment trap opening (0.5 m^2). The same calculation was carried out for PN.

An additional two splits were taken for analysis of $\delta^{13}C_{POC}$ and $\delta^{15}N_{PN}$. These samples were processed as above for POC and PN but were analysed on a Thermo Finnigan Delta-Plus Advantage isotope ratio mass spectrometer. All $\delta^{13}C_{POC}$ and $\delta^{15}N_{PN}$ data are presented as delta per mille (‰) enrichment relative to a standard,

$$\delta X(‰) = 10^3\left(R_{sample}/R_{standard} - 1\right) \quad (2)$$

where *R* denotes the $^{13}C/^{12}C$ ratio for carbon or the $^{15}N/^{14}N$ ratio for nitrogen. $R_{standard}$ refers to the international standard used as reference material for $\delta^{13}C$ and $\delta^{15}N$ which is Vienna Pee Dee belemnite (V-PDB) and atmospheric nitrogen (AIR) respectively, both of which were calibrated against the PACS international standard. Multiple repeats of analytical standards gives a reproducibility of 0.2‰ for C and N, smaller than the possible effects of formalin preservation (±1‰ and ±1.5‰ for C and N respectively) (Mincks et al., 2008 and refs. within).

https://doi.org/10.5194/bg-2022-246
Preprint. Discussion started: 4 January 2023

192

193 *2.3.2. Biogenic silica*

194 Two splits were taken for each sample (from both deep and shallow sediment traps) for analysis of
195 biogenic silica and silicon isotopes. Split material was filtered onto 25 mm, 0.4 µm, polycarbonate
196 filters and rinsed with Mili-Q water before drying at 50 °C for 24h. Material on the filters was
197 solubilised via an alkaline extraction method (Hatton et al., 2019) carried out at the Bristol Isotope
198 Group (BIG) laboratory. Sample material was digested in Teflon tubes with 0.2M NaOH at 100 °C for
199 40 minutes. This was followed by neutralisation with 6M HCl. Biogenic silica ($BiSO_2$, termed BSi)
200 concentrations were measured chlorometrically by molybdate blue spectrophotometry (Heteropoly
201 Blue Method) (Strickland and Parsons, 1972) using a Hach DR3900 spectrophotometer. Supernatants
202 were stored for 7-11 months before column chemistry for isotope analysis. Fluxes of biogenic silica
203 were calculated as for POC using equation 1.

204 For Si isotope analysis, supernatants and reference standards were purified by passing through pre-
205 cleaned cation exchange columns (Bio-Rad AG50W-X12, 200-400 mesh resin) following (Georg et al.,
206 2006) using HCl as eluent. Samples were acidified to a pH of 1-2 to ensure that all the silicon
207 remained in solution. Samples were loaded onto columns and eluted with Milli-Q water to produce a
208 2.5 ppm solution, and concentrations checked to confirm quantitative yields. Si isotopic composition
209 was analysed within 24 hours of column chemistry. Stable Si isotopic compositions were measured
210 at the BIG laboratory on a Finnigan Neptune Plus High-Resolution MC-ICP-MS (Thermo Fisher
211 Scientific). The Si solutions were spiked with magnesium spike (Inorganic Ventures MSMG-10 ppm),
212 hydrochloric acid (1M HCl in-house distilled) and sulphuric acid (0.1M H_2SO_4, ROMIL-UpA™ Ultra
213 Purity Sulphuric Acid), and transferred from the autosampler via a PFA Savillex C-Flow nebuliser (35
214 µl min^{-1}) connected to an Apex IR Desolvating Nebulizer (Ward et al., 2022), and measured on the
215 low-mass side to resolve any isobaric interferences (e.g., $^{14}N^{16}O^+$). All standards and samples were
216 blank corrected offline. The intensity of ^{28}Si in the 0.1M HCl blank was <1% of the sample intensity in
217 all sample runs. Furthermore, we also measured Mg isotopes (^{24}Mg, ^{25}Mg and ^{26}Mg) as an internal
218 isotopic reference to correct for any mass-dependent fractionation (White et al., 2000).
219 Measurements that resulted in large corrections (>0.3‰ on $\delta^{30}Si$) underwent repeat analysis.
220 Instrumental mass bias was further accounted for using a standard-sample bracketing method using
221 a 2 ppm reference standard (NBS or RM8546) solution. Two samples were analysed for each
222 sediment trap bottle (pseudo replicates as the sediment trap material was heterogeneous), as well
223 as standards and sample blanks. Solutions were measured in replicate (n = 2-3) alongside continuous
224 measurement of reference standards Diatomite and LMG-08 to ensure reproducibility and to
225 monitor data quality. Measurements of Diatomite and LMG-08 yielded $\delta^{30}Si$ of +1.23‰ (SD ± 0.03,
226 n=18) and -3.40‰ (SD ± 0.05, n=5) respectively, which agreed with published values (Reynolds et al.,
227 2007; Hendry and Robinson, 2012; Grasse et al., 2017). Typical reproducibility between the sample
228 pseudo replicates was 0.04‰ (1 x SD).

229 *2.4. Chlorophyll and phytoplankton community composition*

230 Surface chlorophyll concentrations were obtained from Ocean Colour CCI (version 5.0)
231 (Sathyendranath et al., 2021, 2019). We present the mean of 8-day concentrations for December
232 2018 as well as the seasonal cycle of 8 day chlorophyll concentrations averaged over a 1 x 1°
233 bounding box around our study site (–41 °E, -40 °E, -53 °N, -52 °N).

https://doi.org/10.5194/bg-2022-246
Preprint. Discussion started: 4 January 2023

Phytoplankton and microzooplankton community composition of a small selection of samples from the two main productive periods, were assessed via light microscope. A biological method of sample preparation and analysis was chosen, comparable with Rembauville et al. (2015), to determine the quantity of empty and full diatom cells. Following subsampling using the rotary splitter, samples for morphological taxonomic analysis were diluted to a standardised 25ml. Samples were gently homogenised and 2 ml withdrawn using a modified pipette with widened opening. Several common diatoms in Antarctic waters are long and slim; in particular, *Thalassiothrix antarctica* has been recorded with an apical axis up to 5mm. To ensure such specimens remain intact and are not excluded from the pipetting process, a wide bore opening is necessary. The 2 ml subsamples were used to fill a 1 ml Sedgwick Rafter counting chamber. Chambers were viewed using a compound light microscope (Nikon Eclipse 80i) with differential interference contrast at x200 magnification. For the larger, easily identifiable cells, the whole chamber was observed; for smaller cells a proportion of the chamber was examined depending upon cell abundance (at least 500 cells were counted). Only complete cells were enumerated to avoid over counting of fragmented specimens. Cells were determined as "full" or alive at time of collection if they possessed chloroplasts/plastids, pigment, a nucleus or, in the case of *Pronoctiluca*, a distinct accumulation body; cells lacking these internal features were deemed as "empty", or dead at time of collection. Specimens were identified according to Hasle and Syvertsen (1997); Medlin and Priddle (1990); Priddle and Fryxell (1985) and Scott and Marchan (2005).

Cell bio-volume and surface area estimates were calculated using geometrics and related equations for phytoplankton genera proposed by Hillebrand et al. (1999). Metrics used in the calculations were based on the average size of ten randomly selected specimens belonging to a species/taxonomic group within the samples.

3. Results

3.1. Environmental conditions

Mean current velocities were 0.11 (±0.06) and 0.06 (±0.03) m s^{-1} for shallow and deep current meters respectively (Supplementary Figure S1). Maximum current speeds recorded reached 0.43 and 0.18 m s^{-1} for shallow and deep meters respectively. The periods with currents substantially elevated above the mean were June for both traps, and additionally in late August/September for the shallow trap, both for periods of ~5-10 days. Both are periods of low fluxes during austral winter and are not the main subject of the study here, though it is likely that particle collection was biased at these times (Buesseler et al., 2007).

Satellite derived estimates of surface chlorophyll show high concentrations during austral summer (January to March) peaking at 2.3 mg m^{-3}, as well as during spring (November-December), peaking at 2.1 mg m^{-3} (Figure 2, Figure S2). Data coverage is limited in the winter due to cloud cover, but concentrations appear to be <1 mg m^{-3}. We define here two productive periods (when chlorophyll concentrations were >0.4 mg m^{-3}), which we refer to throughout the manuscript, productive period 1: January to April 2018, and productive period 2: September to December 2018.

https://doi.org/10.5194/bg-2022-246
Preprint. Discussion started: 4 January 2023

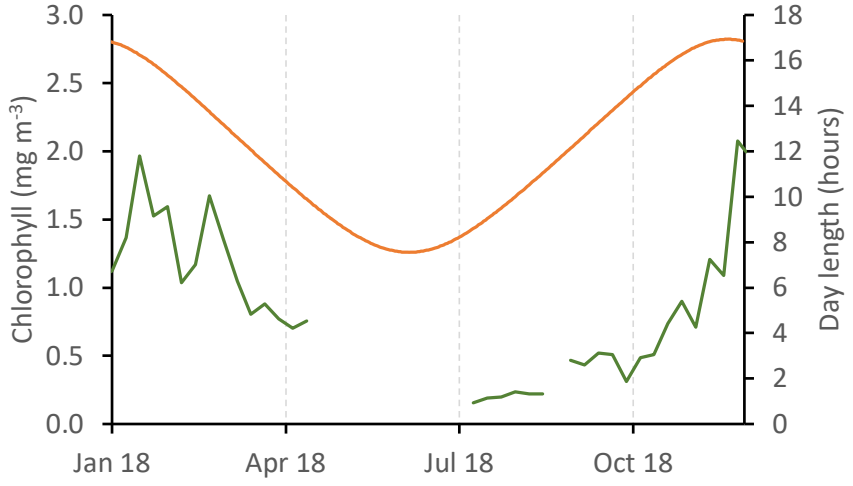

Figure 2: Seasonal cycle of satellite derived surface chlorophyll concentration (green line, 8 day data from the Ocean Colour CCI (version 5.0) (Sathyendranath et al., 2021, 2019)***. Daylength at -53 °N is shown by the orange line.***

3.2. POC, PN, BSi fluxes

There is a clear seasonal cycle in POC, PN and BSi fluxes, all tracking each other well (Figure 3). POC fluxes were low during austral autumn and winter, with mean fluxes <10 mg C m^{-2} d^{-1} and <7 mg C m^{-2} d^{-1} for shallow and deep traps respectively during the period March to October 2018. Higher fluxes were measured in summer 2018 (productive period 1), reaching means of 25.3 mg C m^{-2} d^{-1} in late January 2018 in the shallow trap and 13.1 mg m^{-2} d^{-1} in late February in the deep trap. The maximum POC fluxes measured occurred in early December 2018 (productive period 2) with mean POC fluxes of 45.7 mg C m^{-2} d^{-1} and 43.4 mg C m^{-2} d^{-1}, in shallow and deep traps respectively. PN fluxes follow the same trends as POC fluxes, peaking at 4.2 and 2.4 mg N m^{-2} d^{-1} during period 1, and 10.8 and 8.2 mg N m^{-2} d^{-1} during period 2, in shallow and deep traps respectively (Figure 3B).

BSi fluxes (Figure 3C) track those of POC well. Lowest fluxes (<20 mg SiO_2 m^{-2} d^{-1}, except a small peak of up to 39.7 mg SiO_2 m^{-2} d^{-1} in May 2018) occurred in the autumn/winter (March-October). During summer 2018 (productive period 1) BSi fluxes were high, reaching mean fluxes of 129.1 mg SiO_2 m^{-2} d^{-1} in early February in the shallow trap and, 84.3 mg SiO_2 m^{-2} d^{-1} in late February in the deep trap. By far the highest fluxes were observed in spring 2018 (productive period 2), peaking in early December at a mean of 562.4 mg SiO_2 m^{-2} d^{-1}, and 285.4 mg SiO_2 m^{-2} d^{-1} in shallow and deep traps respectively.

The match in timing of sharp peaks in POC, PN and BSi fluxes in the shallow and deep traps in spring (period 2) highlights that sinking rates must be sufficient (>114 m d^{-1}) to travel the 1600 m between the two traps in the 14 day period that the sediment trap cup was open. In period 1, there was a time lag of 14 to 35 days (based on the sampling duration of each sample bottle was open) between the timing of the maximum POC, PN, and BSi fluxes in the deep and shallow sediment traps. This

https://doi.org/10.5194/bg-2022-246
Preprint. Discussion started: 4 January 2023

300 suggests sinking rates of 46-114 m d^{-1}. However, we stress that this assumes vertical sinking, which
301 as we discuss in the Section 4 is not always the case.

https://doi.org/10.5194/bg-2022-246
Preprint. Discussion started: 4 January 2023

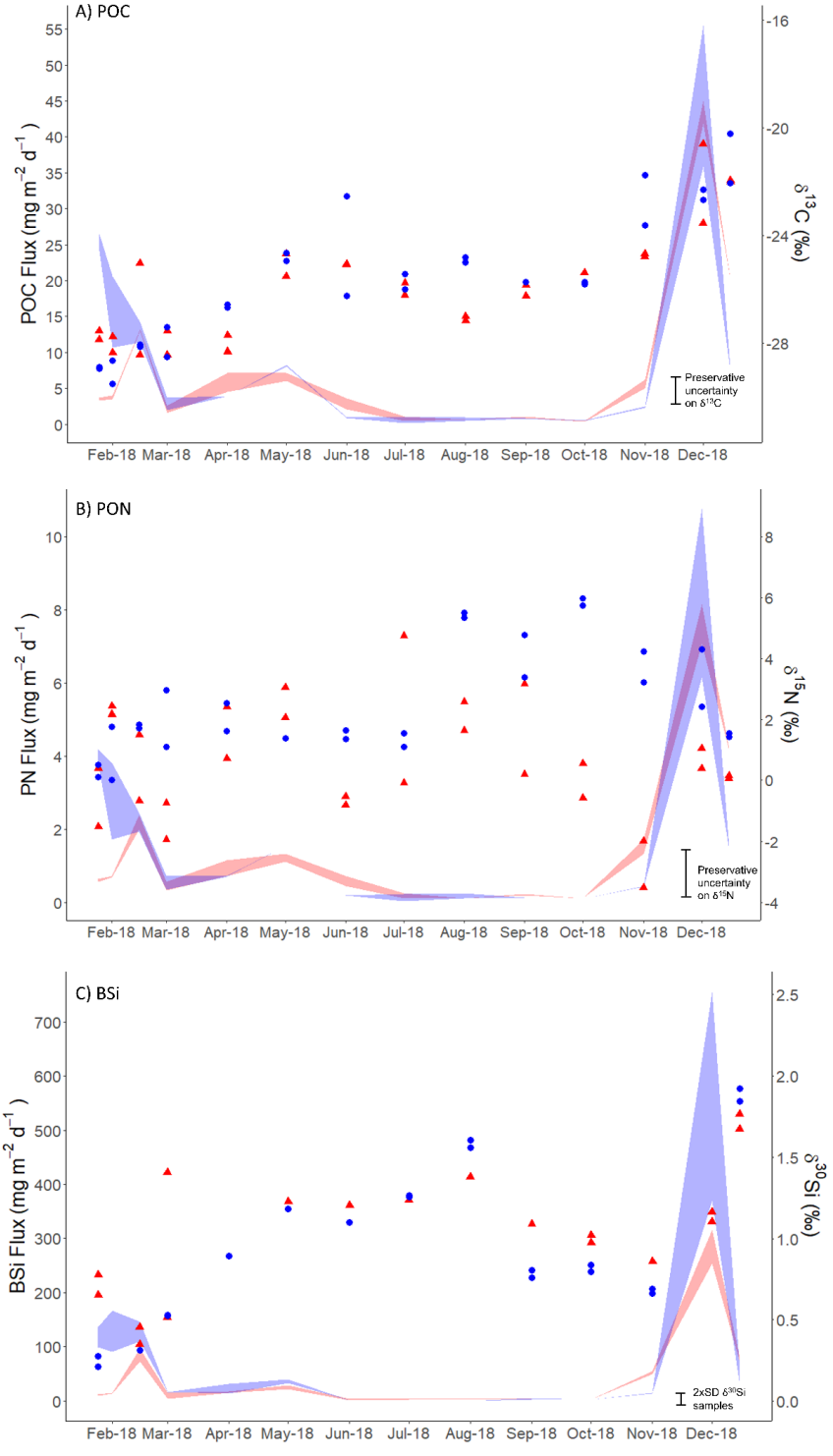

302

https://doi.org/10.5194/bg-2022-246
Preprint. Discussion started: 4 January 2023

Figure 3: A) Particulate organic carbon (POC), B) particulate nitrogen (PN) and C) biogenic silica (SiO_2, BSi) fluxes (mg m^{-2} d^{-1}) at deep (red shading) and shallow (blue shading) sediment traps. Shading indicates the maximum and minimum flux from two replicate samples. Coloured points show isotope ratios for A) $\delta^{13}C_{POC}$, B) $\delta^{15}N_{PN}$ and C) $\delta^{30}Si_{BSi}$ with red triangles and blue circles indicating shallow and deep sediment traps, respectively. The maximum error on sediment trap $\delta^{13}C_{POC}$ (±1‰) and $\delta^{15}N_{PN}$ (±1.5‰) values are shown by scaled error bars and are associated with formaldehyde preservation (Mincks et al., 2008) since this vastly exceeds analytical error. For $\delta^{30}Si_{BSi}$, the scaled error bar represents 2 x SD (‰0.7) for the analytical sample replicates. For each sample fluxes and isotope ratios are given at the date that sample cup was opened.

3.3. $\delta^{13}C_{POC}$, $\delta^{15}N_{PN}$ and $\delta^{30}Si_{BSi}$ Isotopes

$\delta^{13}C_{POC}$ values of deep and shallow sediment trap samples track each other well and show the same order of enrichment/depletion (Figure 3A). Initially, from January to March 2018, we see isotopically light mean $\delta^{13}C_{POC}$ values between -27.40 and -28.56‰, before increasing to -24.38‰ and -25.07‰ in June in shallow and deep traps respectively. Over winter, $\delta^{13}C_{POC}$ became more depleted (shallow: -25.76‰ in October, deep -27.07‰ in August) with a slight divergence (2.17‰) in the tracking of deep and shallow $\delta^{13}C_{POC}$ in August 2018. Coinciding with increasing chlorophyll concentrations, $\delta^{13}C_{POC}$ became more enriched during the period September to December 2018 (-25.72 to -21.13‰ and -26.04 to -21.98‰ for shallow and deep traps respectively).

Comparison of flux weighted $\delta^{13}C_{POC}$ values confirms the carbon isotopic similarity of deep and shallow traps, particularly during period 2 (Table 1). These results also highlight the baseline shift in both $\delta^{13}C_{POC}$ and $\delta^{30}Si_{BSi}$ between period 1 and period 2.

Table 1: Sediment trap seasonal (Jan 2018-Dec 2018), period 1 (Jan 2018 – April 2018), and period 2 (Sept 2018-Dec 2018) flux weighted mean $\delta^{13}C_{POC}$ (‰), $\delta^{15}N_{PN}$ (‰) and $\delta^{30}Si_{BSi}$ (‰) for shallow (400 m) and deep (2000 m) traps. Maximum errors are based on uncertainty associated with formaldehyde preservative and analytical sample replicates.

	$\delta^{13}C_{POC}$ (‰)		$\delta^{15}N_{PN}$ (‰)		$\delta^{30}Si_{BSi}$ (‰)	
Time period	Shallow	Deep	Shallow	Deep	Shallow	Deep
Seasonal	-25.14 ±1‰	-24.39 ±1‰	2.53 ±1.5‰	0.38 ±1.5‰	0.89 ±0.07‰	1.08 ±0.07‰
Period 1	-28.31 ±1‰	-27.54 ±1‰	1.34 ±1.5‰	0.74 ±1.5‰	0.47 ±0.07‰	0.52 ±0.07‰
Period 2	-22.50 ±1‰	-22.85 ±1‰	3.45 ±1.5‰	-0.07 ±1.5‰	1.28 ±0.07‰	1.19 ±0.07‰

$\delta^{15}N_{PN}$ values are less consistent between deep and shallow sediment trap samples and there is more heterogeneity between sample replicates. For the shallow trap we see values ranging between +0.13 and +2.96‰ (mean +1.42‰, SD 0.79‰) from January to June 2018, and, for the deep trap, values ranged between -1.95 and +3.04‰ (mean +0.60‰, SD 1.60‰) during this period. There is no clear trend during this period, but shallow and deep traps have $\delta^{15}N_{PN}$ of similar magnitude. Values increase between June and August, reaching a mean of +5.42 and +2.10‰ in shallow and deep traps respectively. From August to December (shallow), and August to November (deep), we see a trend of decreasing $\delta^{15}N_{PN}$ to +1.49 and -2.77‰ in shallow and deep traps respectively. Shallow $\delta^{15}N_{PN}$ are

https://doi.org/10.5194/bg-2022-246
Preprint. Discussion started: 4 January 2023

consistently higher than deep $\delta^{15}N_{PN}$ by 4.52‰ on average during this period (August to November). In the deep trap we see a final increase in $\delta^{15}N_{PN}$ coinciding with the increase in PN flux from November to December 2018, reaching a mean of +0.71‰. The same increase in $\delta^{15}N_{PN}$ is not apparent in the shallow trap.

Si isotope compositions in deep and shallow samples were similar, exhibiting the same seasonal patterns. Both deep and shallow traps showed an increase in $\delta^{30}Si_{BSi}$ from January to July 2018 (+0.24 to +1.26‰) with the steepest increase occurring from March to May (Figure 3C). Sample replicates generally showed good agreement with one exception during March 2018 when duplicate samples from the deep sediment trap were +0.52 and +1.41‰ highlighting the heterogeneous nature of the sediment trap material. Isotopic values were then quite steady over winter until the end of August when $\delta^{30}Si_{BSi}$ began to decrease steeply, reaching +0.68 and +0.86‰ in shallow and deep traps respectively in November 2018. Following this, $\delta^{30}Si_{BSi}$ increased rapidly to +1.72 (deep) and +1.89‰ (shallow) coinciding with the large increase in BSi fluxes at this time.

3.4. Phytoplankton community structure

Eight samples (four deep and four shallow) were analysed microscopically for phytoplankton composition to cover the high productivity periods 1 and 2. Only intact cells were identified and counted. In terms of abundance, during period 1 *Fragilariopsis spp.* dominated both deep (58-66%) and shallow (~70%) trap samples (Figure 4A, B), whereas during period 2 the phytoplankton community structure was more mixed with contributions from *Thalassionema nitzshiodes, Chaetoceros,* small (<20 µm) centrics, as well as *Fragilariopsis spp.* Large centrics (>20 µm) represented 15-20% of the community by abundance in the deep trap during productive period 1, but <2.5% in productive period 2. Interestingly we do not see these large centrics in the shallow trap during productive period 1, implying that sinking velocities were < 76 m d^{-1} for these large phytoplankton cells.

In terms of biovolume, *Fragilariopsis spp.* were still a dominant component of the shallow trap sample in period 1 (~33%) but were <9% of the community in the deep trap during period 1, with the large cells of *Coscinodiscus* dominating 39-67% (Figure 4C, D). *Corethron pennatum* (shallow: 10-13%; deep: 15%), *Rhizosolenia* (shallow: 9-21%), large centrics (>20 µm) (shallow: 10-17%; deep: 16-20%), and *Dictyocha* (shallow: 9-10%; deep: 8%) were also relatively high in terms of biovolume during period 1. During period 2, the community in terms of biovolume was quite mixed in the shallow trap (Figure 4C), with similar contributions from *Fragilariopsis spp.* (22-28%), *Dictyocha* (14-15%), *Coscinodiscus* (10%), and, small (<20µm, 9-14%) and large centrics (>20µm, 9-19%) in the deep trap.

https://doi.org/10.5194/bg-2022-246
Preprint. Discussion started: 4 January 2023

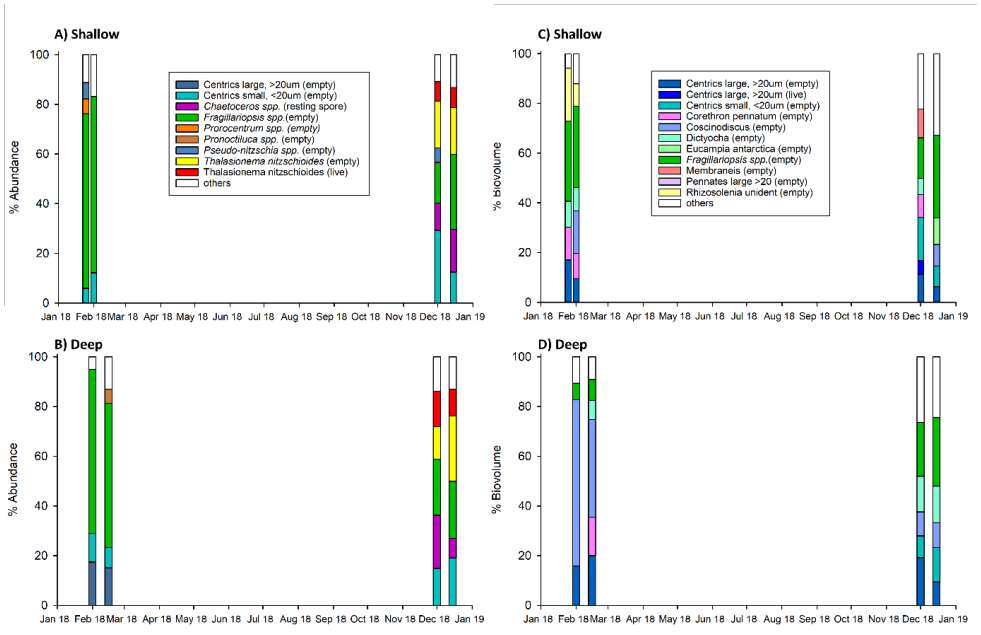

372 ***Figure 4: Phytoplankton assemblage of A,C) shallow and B, D) deep sediment trap samples. Four***
373 ***samples were taxonomically identified for each trap. Shown here are the phytoplankton***
374 ***contributing >5% by abundance (A,B) or >5% by biovolume (C,D). Note that only intact cells were***
375 ***counted.***

376

https://doi.org/10.5194/bg-2022-246
Preprint. Discussion started: 4 January 2023

4. Discussion

In this study we measure the seasonal cycle of POC, PN and BSi fluxes as well as the $\delta^{13}C_{POC}$, $\delta^{15}N_{PN}$ and $\delta^{30}Si_{BSi}$ values of sinking particles collected in shallow (400 m) and deep (2000 m) sediment traps in the Scotia Sea, Southern Ocean. Both the magnitude and isotopic compositions were generally similar in the shallow and deep sediment traps, suggesting that most remineralisation occurred in the upper 400 m. This highlights that material reaching 400 m likely facilitates the transfer of carbon much deeper in the ocean, sequestering carbon for longer time periods.

4.1. Seasonal flux cycles

Seasonal cycles of POC agree well with previously published work at the same location (Manno et al., 2015) with peaks in austral spring and late summer; though the peak POC fluxes recorded here (means of 45.7 mg C m^{-2} d^{-1} and 43.4 mg C m^{-2} d^{-1}, in shallow and deep traps respectively) are higher than those observed in previous years (22.9 mg C m^{-2} d^{-1}; Manno et al. (2015)). A smaller third peak in POC flux (<10 mg C m^{-2} d^{-1}) occurred in April/May, in agreement with some previous years (Manno et al., 2015). PN fluxes followed the same seasonal trend as POC. The fluxes of BSi observed here are higher than previously observed at this site at 2000 m in 2012 (Rembauville et al., 2016). Maximum fluxes of 46.0 mg SiO_2 m^{-2} d^{-1} were recorded by Rembauville et al. (2016) in January 2012, which though of similar magnitude to our summer peak of 84.3 mg SiO_2 m^{-2} d^{-1}, is an order of magnitude lower than the spring peak of 285.4 mg SiO_2 m^{-2} d^{-1} in December 2018. However, the Rembauville et al. (2016) record ends in November and therefore would not have captured the main peak in particle flux following the phytoplankton spring bloom in December (apparent in satellite surface chlorophyll, Figure 2 in Rembauville et al. (2016)). Closset et al. (2015) measured very high fluxes (>700 mg SiO_2 m^{-2} d^{-1}) of BSi south of the Polar Front in the Australian sector of the Southern Ocean at 2000 m, and similarly high fluxes have been observed in other sectors (Fischer et al., 2002; Honjo et al., 2000).

We define two main productive periods, productive period 1 from January to April 2018, and productive period 2 from September to December 2018 when chlorophyll concentrations were >0.4 mg m^{-3}. The particle fluxes associated with productive period 2 were much higher than those during productive period 1, a difference which is particularly pronounced for BSi fluxes. The bloom during period 2 was more geographically widespread (Figure S2) and thus it is possible that if more of the material reaching the trap was sourced from productive waters, this could have supported the higher fluxes observed at this time. The observed higher BSi fluxes in productive period 2 could also relate to, the presence of more heavily silicified diatom species at this time, including the occurrence of resting spores (*Chaetoceros spp.* Figure 4, and Rembauville et al. (2016)), increased aggregation (and thus sinking) potential, and/or reduced grazing pressure. The fact that we observed resting spores at the end of productive period 2, suggests that nutrients may have started to become limiting for at least some of the phytoplankton community (e.g. silicic acid and/or iron (Rembauville et al., 2016). Satellite data suggest the magnitude of chlorophyll concentration was similar during both productive periods, but increasing in magnitude throughout period 2, and decreasing in period 1. POC and BSi fluxes track each other closely, which combined with our visual observations of a dominance of algal material in the trap during the spring peak (dominated by diatoms, Figure 4), highlights the role of diatoms in transferring organic carbon to the deep ocean. This could be achieved through their greater density, and thus sinking velocities, associated with mineral (silica)

https://doi.org/10.5194/bg-2022-246
Preprint. Discussion started: 4 January 2023

ballast, or through the bioprotection of internal organic matter from grazing and oxidation of the silica frustules (Passow and De La Rocha, 2006; Armstrong et al., 2001; Smetacek et al., 2004).

4.2. Seasonal shifts in isotope ratios

In terms of the seasonality, we see broadly similar trends for both $\delta^{13}C_{POC}$ and $\delta^{30}Si_{BSi}$ (linear regression, $R^2 = 0.452$, $P<0.001$), again highlighting the close coupling of carbon and silicon cycling processes. During productive period 1, $\delta^{13}C_{POC}$ is low, averaging -28.31 and -27.54‰ in shallow and deep traps respectively, close to that expected for Southern Ocean phytoplankton employing typical C3 metabolism (i.e. diffusive CO_2 transfer into the internal cell pool and Rubisco carboxylation) (Raven, 1997). This is supported by the dominance of *Fragilariopsis spp.* in the trap material, as Bacillariophyceae are known to employ C3 metabolism (Table IV in Raven, 1997)**.** Preferential uptake of ^{28}Si by diatoms (De La Rocha et al., 1997) during the late spring bloom of productive period 1, also explains the low $\delta^{30}Si_{BSi}$ values. After initial low values, we see a progressive increase in both $\delta^{13}C_{POC}$ and $\delta^{30}Si_{BSi}$, reflecting the progressive utilisation of both ^{12}C and ^{28}Si as nutrient pools are consumed during the bloom. As such, the diatom cells reaching the sediment trap in late spring/summer were utilising increasingly isotopically-enriched C and Si for growth leading to progressive isotopic enrichment of the cells sinking into the sediment trap. This observation fits with elevated but decreasing surface chlorophyll concentrations from February to April 2018. Increasing $\delta^{13}C_{POC}$ and $\delta^{30}Si_{BSi}$ into the late summer may also partially reflect preferential remineralisation of the more labile ^{12}C and ^{28}Si in particles as they sink through the upper 400 m of the water column. Though the lack of variation in $\delta^{13}C_{POC}$ and $\delta^{30}Si_{BSi}$ between 400 and 2000 m in our study suggests this may be limited over these depth ranges, or that there is no fractionation effect. Whilst laboratory-based silica dissolution experiments are equivocal (Demarest et al., 2009; Wetzel et al., 2014), our findings agree with field studies that also indicate a lack of Si isotopic fractionation during diatom silica dissolution (Closset et al., 2015; Egan et al., 2012).

Between May and August, both $\delta^{13}C_{POC}$ and $\delta^{30}Si_{BSi}$ were consistent, with a slight progressive decrease for $\delta^{13}C_{POC}$ and slight increase in $\delta^{30}Si_{BSi}$. It is possible that the slight progressive trend towards a lighter carbon isotopic composition of sinking particles from -24.94 to -25.98‰ is driven by a mixture of older, isotopically heavier particles that have undergone partial remineralisation and the input of fresher material from the small secondary peak in POC we observed in April/May. Either the small autumn peak consisted of a different phytoplankton community, or we are seeing a signal of smaller, more slowly sinking cells reaching the trap in increasing numbers following the initial late spring peak in production. Korb et al. (2012) found an increasing presence of dinoflagellates from spring to summer, as well as seasonal changes in the size structure of the phytoplankton community to the northwest of South Georgia, supporting either hypothesis. We do not have the species composition data from this time period to evidence this directly, but we suggest that the reduction in $\delta^{13}C_{POC}$ does not relate to a mixing event and a resupply of ^{12}C, due to the fact that $\delta^{30}Si_{BSi}$ continued to increase slowly. Given the generally lighter silicon isotopic composition of seawater below the photic zone, we would expect a mixing event to also result in a decline in seawater $\delta^{30}Si$ and, so, $\delta^{30}Si_{BSi}$. This would mean that our hypothesised shift in phytoplankton species composition in the traps (May-August) did not impact Si fractionation to the same extent as carbon isotopes. Whereas size, growth rates, cell geometry and different carbon acquisition mechanisms have all been highlighted as impacting the $\delta^{13}C_{POC}$ of marine plankton (Popp et al., 1999, 1998; Bidigare et al., 1999; Trull and Armand, 2001; Tuerena et al., 2019), species dependent Si fractionation by polar and

https://doi.org/10.5194/bg-2022-246
Preprint. Discussion started: 4 January 2023

462 subpolar diatoms has only been observed in the laboratory, not in the field (Annett et al., 2017;
463 Cassarino et al., 2017; Sutton et al., 2013).

464 During the summer-autumn period (January- June 2018), there was no clear trend in $\delta^{15}N_{PN}$, with
465 values between -1.94 and +3.04‰. We speculate that this mixed signal with no significant difference
466 between deep and shallow traps resulted from a combination of surface phytoplankton using both
467 ammonium and nitrate, and variability in the sediment trap material composition, for example the
468 presence of faecal pellets, as well as animal moults and carcasses. Enrichments of 2-4‰ occur
469 between successive trophic levels, and egestion and excretion can have varying isotopic effects (see
470 Section 4.3). Additionally, any supply of ammonium through remineralisation would be utilised
471 quickly because ammonium is kinetically favourable to nitrate (Glibert et al., 2016), resulting in
472 particles with a decreased $\delta^{15}N_{PN}$ compared to those produced by nitrate assimilation.

473 Between August and September we saw a sharp decrease in $\delta^{30}Si_{BSi}$ (~0.5‰) in both traps suggesting
474 resupply of ^{28}Si enriched silicic acid to the euphotic zone via mixing. Interestingly, we did not see the
475 same consistent shift in carbon isotopes; we measured a ~1‰ decrease in the shallow trap $\delta^{13}C_{POC}$
476 and a ~1‰ increase in the deep trap $\delta^{13}C_{POC}$. We speculate that this mixing could bring waters of
477 increased silicic acid concentrations to the surface, supporting lower δ^{30}BSi in sinking particles
478 following phytoplankton uptake, but that the mixed waters were similar in dissolved inorganic
479 carbon concentrations and $\delta^{13}C$. This could relate to the depth of mixing and differences in the depth
480 at which POC and BSi are remineralised (Friedrich and Rutgers van der Loeff, 2002; Weir et al., 2020).
481 We note that current velocities recorded at this time were elevated (Figure S1), particularly in the
482 deep trap, suggesting a shift in the surrounding velocity fields, and may also have resulted in biased
483 sample collection at this time through over or under collection (Buesseler et al., 2007). Whereas
484 $\delta^{13}C_{POC}$ progressively increased during productive period 2, from -25.88‰ in September to -21.56‰
485 at the end of December, $\delta^{30}Si_{BSi}$ continued to decrease until November before showing a sudden
486 increase from +0.74‰ to +1.80‰ at the end of the sampling period. This may suggest that DSi (or
487 co-limiting nutrients) was replete, and uptake could occur unhindered until November 2018 when
488 very high rates of production and the associated high fluxes of BSi increased the demand for DSi, and
489 led to enrichment of $\delta^{30}Si$ in overlying waters and subsequently sinking siliceous phytoplankton. For
490 carbon, uptake was sufficient from September 2018 to progressively deplete source waters (and
491 subsequent newly formed phytoplankton cells) in ^{12}C.

492 $\delta^{15}N_{PN}$ decreased progressively from August to December, though the deep sediment trap showed a
493 sharp increase from a mean of -2.77 to +0.71‰ at the start of December, before decreasing again.
494 The progressive decrease is consistent with the propagation of the surface signal of phytoplankton
495 growth and fractionation, with increasing influence of ammonium uptake that leads to low $\delta^{15}N_{PN}$.
496 Interestingly, unlike C and Si isotopes, we saw a divergence in the nitrogen isotopic composition of
497 deep and shallow traps during this period. Though they mostly followed the same decreasing trend,
498 the trend in the shallow trap was less pronounced and started from a higher mean value of +5.42‰.
499 The sharp increase in mean $\delta^{15}N_{PN}$ from +1.32‰ in July to +5.42‰ in August 2018 in the shallow
500 trap that initiated the divergence strongly suggests an advective change in source material. As noted
501 above, this was a period of increased horizontal velocities and may have facilitated material reaching
502 the two traps from different sources of differing initial composition and degradation states. The
503 substantially lower $\delta^{15}N_{PN}$ in the deep trap from August to November, compared to that of the
504 shallow trap is surprising given that we would expect progressive decomposition of particles to

https://doi.org/10.5194/bg-2022-246
Preprint. Discussion started: 4 January 2023

505 remove dissolved nitrogen depleted in ^{15}N. This would increase $\delta^{15}N_{PN}$ in the particles, and indeed
506 many studies have observed this trend of increasing $\delta^{15}N$ with depth in suspended particles (Altabet
507 et al., 1991 and refs. within). However, like Altabet et al. (1991), we observe lower $\delta^{15}N_{PN}$ in sinking
508 particles in the deep sediment trap. This has also been observed previously in Antarctic waters
509 (Wada et al., 1987). Though the reason for this is not well understood (Sigman and Fripiat, 2019), it
510 appears to be a consistent phenomenon. Particles in our deep trap must therefore be gaining light
511 nitrogen or losing heavy nitrogen and could reflect a different source composition. In agreement
512 with Altabet et al. (1991), we suggest that lateral transport of low $\delta^{15}N_{PN}$ from a region of increased
513 ammonium based production could explain this, highlighting a difference in the source of sinking
514 particles to the two traps. Altabet et al. (1991) also suggest that, since protein nitrogen is 3‰ higher
515 than bulk nitrogen, the selective decomposition of protein could explain the decrease in $\delta^{15}N$ with
516 depth, though why this would not be the case also for suspended PN is unclear. We observe the
517 greatest divergence in shallow and deep N isotope compositions during periods of low PN flux
518 (Figure 3, consistent with the observations of Altabet et al. (1991)), enabling a low flux of laterally
519 supplied material to have an amplified impact on the isotope signal. In support of this, in December
520 when particle fluxes increase sharply with the spring bloom, $\delta^{15}N_{PN}$ in the deep trap increases more
521 in line with that of the shallow trap, highlighting a switch from source material being dominated by
522 lateral supply when vertical supply is negligible, to the dominance of vertical supply from surface
523 production.

524 Though complex, it is clear that seasonal patterns in isotopic composition of particulate material
525 reaching the sediment traps closely reflects the degree and type of nutrient utilisation in the source
526 waters. As we capture two main productive periods in our study, we can more closely examine the
527 different isotopic baselines observed in these two periods.

528 *4.3. Drivers of a shifting isotopic baseline*

529 Productive periods 1 (January to April 2018) and 2 (September to December 2018) exhibit differing
530 baselines in their isotopic composition (Figure 3, Table 1). The divergence in the $\delta^{15}N_{PN}$ of deep and
531 shallow trap material during period 2 limits our ability to compare baselines for nitrogen isotopes, so
532 we focus here on $\delta^{13}C_{POC}$ and $\delta^{30}Si_{BSi}$. Since our record does not extend beyond December 2018, we
533 cannot determine if $\delta^{13}C_{POC}$ and $\delta^{30}Si_{BSi}$ would return to values akin to that in period 1 in the
534 following late spring-summer season (January 2019). We saw a shift in the baseline $\delta^{13}C_{POC}$ from a
535 mean of -28.31‰ in January 2018 at the start of period 1, to -25.88‰ in September at the start of
536 period 2. This coincided with a change in community structure, with abundance dominated by
537 *Fragilariopsis spp.* in period 1 to a more mixed community in period 2. Of the abundant
538 phytoplankton species (>5%, Figure 4A, B) we find statistically significant linear relationships
539 between $\delta^{13}C_{POC}$ and percent abundance for *Fragilariopsis spp.* (empty: $R^2 = 0.926$, $p<0.001$),
540 *Thalassionema nitzschioides* (live: $R^2 = 0.774$, $p=0.004$, empty: $R^2 = 0.844$, $p=0.001$), and *Chaetoceros*
541 *spp. (resting spore)* ($R^2 = 0.732$, $p=0.007$). We stress this is based on only 8 samples. Though
542 *Fragilariopsis spp.* were mainly empty cells, colonisation by bacteria (Grossart et al., 2003; Kiørboe et
543 al., 2003) may facilitate carbon transfer within and on these cells, and certainly the live cells of *T.*
544 *nitzschioides* and resting spores of *Chaetoceros spp.* would act as agents of carbon transfer (Agusti et
545 al., 2015; Salter et al., 2012; Rembauville et al., 2016).

546 We examine whether this shift in community composition is associated with a change in SA:V (Table
547 2) since greater fractionation of carbon in smaller phytoplankton cells with higher SA:V is well

https://doi.org/10.5194/bg-2022-246
Preprint. Discussion started: 4 January 2023

observed in the literature (e.g. Popp et al., 1998; Tuerena et al., 2019). There was a statistically significant (paired t-test, p=0.008) difference in the community SA:V between productive periods, increasing from 0.35 $\mu m^2\ \mu m^{-3}$ in period 1 to 0.51 $\mu m^2\ \mu m^{-3}$ in period 2. However, this would act in opposition to the decreased baseline fractionation at the start of period 2 compared to period 1. We note here, that as only intact cells were counted, the measured SA:V ratios may not fully represent the isotopic composition of the trap material due to the presence of fragmented material. It is possible that there was a change in the method of carbon uptake with the more mixed phytoplankton community using HCO_3^- instead of CO_2 or employing carbon concentrating mechanisms (CCM), both of which would result in higher $\delta^{13}C_{POC}$ than the diffusive uptake of CO_2 via Rubisco (Raven, 1997; Cassar et al., 2004). Studies show that there is much diversity amongst diatoms in the use of CCMs and many are able to take up both CO_2 and HCO_3^- (Trimborn et al., 2009; Roberts et al., 2007; Shen et al., 2017; Young et al., 2016). We suggest that species driven differences in carbon uptake mechanisms account in part for the differing baselines in $\delta^{13}C_{POC}$ that we observed at the start of period 1 and period 2.

Table 2: Phytoplankton cell community surface area to volume (SA:V) ratios measured in deep and shallow sediment traps for samples enumerated in both productive periods 1 and 2.

Bottle open date	Depth	Period	Mean community SA:V
25/01/2018	Shallow	1	0.39
01/02/2018	Shallow	1	0.35
01/02/2018	Deep	1	0.33
15/02/2018	Deep	1	0.32
01/12/2018	Deep	2	0.53
15/12/2018	Deep	2	0.53
01/12/2018	Shallow	2	0.48
15/12/2018	Shallow	2	0.52

The fact that we also observed a shifting baseline in $\delta^{30}Si_{BSi}$, and that, with the exception of one culture study, systematic species driven shifts in $\delta^{30}Si_{BSi}$ fractionation have not been observed, suggests that there may be an additional driver of the changing isotopic baselines we observed between the start of period 1 and period 2. Since, prior to our first measurements there had been a long-lasting phytoplankton bloom (Figure S2), we would expect production to have utilised much of the light ^{28}Si, resulting in particles with enriched $\delta^{30}Si_{BSi}$ reaching the trap in January 2018. However, we observe isotopically light mean values of +0.48‰ at the start of period 1, suggesting that there must have been a resupply of ^{28}Si. Physical mixing, bringing deep and benthic waters rich in nutrients, including iron, to the surface waters around South Georgia, are known to support the large blooms occurring downstream of South Georgia (Matano et al., 2020; Nielsdóttir et al., 2012) and could supply both ^{12}C and ^{28}Si. Additional nutrients could also be supplied to our study region by glacial discharge associated with isotopically light silicon isotopic signatures (Matano et al., 2020; Hatton et al., 2019), or benthic fluxes from shelf sediments, likely also releasing isotopically light DSi (Ng et al., 2020). Therefore, we suggest that low values (increased fractionation) of $\delta^{13}C_{POC}$ and $\delta^{30}Si_{BSi}$. during period 1, relate to increased nutrient availability enabling full expression of the isotopic fractionation and thus isotopically light particulate material to reach the sediment trap.

https://doi.org/10.5194/bg-2022-246
Preprint. Discussion started: 4 January 2023

The ocean circulation in our study region is complex and variable on fine spatial and temporal scales, affecting horizontal and vertical velocities. It is clear from the currents measured at the depths of our two traps (Figure S1), that both the direction and magnitude of the flow can vary seasonally and is not necessarily consistent between the two depths. There are thus potentially different source regions for material in the two traps at certain times of the year. We lack the full depth resolution of vertical and horizontal velocity fields and information on sinking rates to confirm this, but previous studies have highlighted variability in the locations of the Subantarctic Circumpolar Current Front and the Polar Front, as well as eddies generated from these fronts, in our study region (Moore et al., 1999; Boehme et al., 2008; Whitehouse et al., 1996). We suggest that variability in ocean current velocities could drive different isotopic baselines in period 1 and 2, through the supply of material to the trap from a different source region with differing nutrient and remineralisation regimes. This would impact nutrient availability including iron supply, uptake and recycling (Hawco et al., 2021; Ellwood et al., 2020), which in turn influences species composition, nutrient utilisation and uptake rates (e.g. Meyerink et al., 2019).

Since trophic transfer is known to impact both carbon and nitrogen isotope compositions of organic matter, the presence of moults and faecal pellets in trap samples are also important to consider. An incubation study focussed on *Euphausia superba* found that the $\delta^{15}N$ of the *E. superba* faecal pellets was always lower than that of the copepods they ingested, though still higher than that of POM (Schmidt et al., 2003), and Tamelander et al. (2006) measured faecal pellets produced by copepods with depleted ^{15}N compared to the algal food source. Though a few studies on temperate and subtropical copepods showed that the faecal material had similar or slightly higher $\delta^{15}N$ than the food source (Altabet and Small, 1990; Checkley and Entzeroth, 1985), there is not a consistent fractionation effect of egestion, for either $\delta^{15}N$ or $\delta^{13}C$, which may relate to compositional differences (protein, carbohydrate, lipid) and their isotopic values (Tamelander et al., 2006). We are therefore not able to determine the impact of faecal pellets or moults on the isotopic composition of our samples. As phytoplankton material dominated at the times of peak flux, we suggest that the importance of faecal pellets and moults may be greater during periods of lower flux, however we cannot rule out their contribution during the bloom periods.

Summary

We observed that the fluxes and isotopic ratios of sinking particulate material well represent the seasonal cycles in productivity and nutrient uptake in surface waters at our study site in the Scotia Sea. We find that, at our study site, most remineralisation occurs in the upper 400 m of the water column, and below this material is altered relatively little. This suggests that particles reaching 400 m likely facilitate the transfer of carbon much deeper in the ocean, sequestering carbon for longer time periods. We find that particulate fluxes of C, N and BSi are typically coupled, and that the degree to which trends in bulk isotopic compositions are coupled provides information on nutrient and remineralisation regimes, and associated shifts in phytoplankton community structure. We suggest that it would be highly informative to conduct particle specific isotope analysis of common particle types in sediment traps such as faecal pellets, phytoplankton detritus and zooplankton moults, to improve our ability to determine the impact of particle flux composition on bulk isotope compositions. Our data also reveals the importance of the lateral supply of material to the sediment traps and suggests seasonal differences in source regions. This highlights the importance of making

https://doi.org/10.5194/bg-2022-246
Preprint. Discussion started: 4 January 2023

synchronous, and full depth resolution measurements of, physical processes such as current strength and direction, to be able to distinguish between spatial and temporal drivers of shifts in species composition, particle flux and isotopic composition. Through more detailed mechanistic understanding of the drivers of POC flux, and biogeochemical cycling, we can improve estimates of the current and future strength of the BCP and the ocean's role as a CO_2 sink.

Data availability

Phytoplankton abundances and biovolume, as well as mean flux and isotopic ratios are available with the following DOI's:

DOI in progress with the British Antarctic Survey Polar Data Centre

Author contributions

AB and CM conceived the study and participated in fieldwork to collect samples. AB conducted laboratory analysis with support from TW, LF, and UD for isotope analysis. MW conducted phytoplankton analysis and provide intellectual input on phytoplankton community composition. SH and KH provided support for isotopic analysis and contributed to the interpretation of the data and implications. All authors contributed text to the manuscript.

Competing Interests

The authors declare that they have no conflict of interest.

Acknowledgements

We are very grateful to the scientists and crew aboard research cruises JR17002 and DY098 for their efforts to deploy and recover the P3 mooring. We thank staff at the Bristol Isotope Group for running and maintenance of the mass spectrometer facilities at the University of Bristol, as well as Colin Chilcott for technical support for C and N analysis at the University of Edinburgh. AB and CM were supported by NC-ALI funding and ecosystems programme. CM was also funded by UKRI FLF project MR/T020962/1. SH was supported by the United Kingdom Natural Environment Research Council through grant NE/K010034/1. UD was supported by the UK NERC through grant NE/P006108/1. LF was supported by a NERC GW4+ DTP studentship and TW by a CSC-UoB Joint Scholarship. We thank Sally Thorpe and Emma Young for insights on the physical oceanographic conditions of the region. Finally, a special thanks to Flo Atherden for her dedicated work picking out swimmers from the shallow sediment trap.

References

Agusti, S., González-Gordillo, J. I., Vaqué, D., Estrada, M., Cerezo, M. I., Salazar, G., Gasol, J. M., and Duarte, C. M.: Ubiquitous healthy diatoms in the deep sea confirm deep carbon injection by the biological pump, Nat. Commun., 6, 1–8, https://doi.org/10.1038/ncomms8608, 2015.

Altabet, M. A. and Small, L. F.: Nitrogen isotopic ratios in fecal pellets produced by marine Zooplankton, Geochim. Cosmochim. Acta, 54, 155–163, https://doi.org/10.1016/0016-

662 7037(90)90203-W, 1990.

663 Altabet, M. A., Deuser, W. G., Honjo, S., and Stienen, C.: Seasonal and depth-related changes in the
664 source of sinking particles in the North Atlantic, Nature, 354, 136–139,
665 https://doi.org/10.1038/354136a0, 1991.

666 Annett, A. L., Henley, S. F., Venables, H. J., Meredith, M. P., Clarke, A., and Ganeshram, R. S.: Silica
667 cycling and isotopic composition in northern Marguerite Bay on the rapidly-warming western
668 Antarctic Peninsula, Deep. Res. Part II Top. Stud. Oceanogr., 139, 132–142,
669 https://doi.org/10.1016/j.dsr2.2016.09.006, 2017.

670 Armstrong, R. A., Lee, C., Hedges, J. I., Honjo, S., and Wakeham, S. G.: A new, mechanistic model for
671 organic carbon fluxes in the ocean based on the quantitative association of POC with ballast
672 minerals, Deep. Res. Part II Top. Stud. Oceanogr., 49, 219–236, https://doi.org/10.1016/S0967-
673 0645(01)00101-1, 2001.

674 Belcher, A., Manno, C., Ward, P., Henson, S. A., Sanders, R., and Tarling, G. A.: Copepod faecal pellet
675 transfer through the meso- and bathypelagic layers in the Southern Ocean in spring, Biogeosciences,
676 14, https://doi.org/10.5194/bg-14-1511-2017, 2017.

677 Belcher, A., Manno, C., Thorpe, S., and Tarling, G.: Acantharian cysts: high flux occurrence in the
678 bathypelagic zone of the Scotia Sea, Southern Ocean, Mar. Biol., 165,
679 https://doi.org/10.1007/s00227-018-3376-1, 2018.

680 Bidigare, R., Hanson, L., Buesseler, K. O., Wakeham, G., Freeman, H., Pancost, R. D., Millero, J.,
681 Steinberg, P., Popp, N., Latasa, M., Landry, R., and Laws, A.: Iron-stimulated changes in 13C
682 fractionation and export by equatorial Pacific phytoplankton: Toward a paleogrowth rate proxy,
683 Paleoceanography, 14, 589–595, https://doi.org/10.1029/1999PA900026, 1999.

684 Boehme, L., Meredith, M. P., Thorpe, S. E., Biuw, M., and Fedak, M.: Antarctic circumpolar current
685 frontal system in the South Atlantic: Monitoring using merged Argo and animal-borne sensor data, J.
686 Geophys. Res., 113, C09012, https://doi.org/10.1029/2007JC004647, 2008.

687 Buesseler, K. O., Antia, A. N., Chen, M., Fowler, S. W., Gardner, W. D., Gustafsson, O., Harada, K.,
688 Michaels, A. F., Rutgers van der Loeff, M., Sarin, M., Steinberg, D. K., and Trull, T.: An assessment of
689 the use of sediment traps for estimating upper ocean particle fluxes, J. Mar. Res., 65, 345–416,
690 https://doi.org/10.1357/002224007781567621, 2007.

691 Cassar, N., Laws, E. A., Bidigare, R. R., and Popp, B. N.: Bicarbonate uptake by Southern Ocean
692 phytoplankton, Global Biogeochem. Cycles, 18, 1–10, https://doi.org/10.1029/2003GB002116, 2004.

693 Cassarino, L., Hendry, K. R., Meredith, M. P., Venables, H. J., and De La Rocha, C. L.: Silicon isotope
694 and silicic acid uptake in surface waters of Marguerite Bay, West Antarctic Peninsula, Deep. Res. Part
695 II Top. Stud. Oceanogr., 139, 143–150, https://doi.org/10.1016/j.dsr2.2016.11.002, 2017.

696 Checkley, D. M. and Entzeroth, L. C.: Elemental and isotopic fractionation of carbon and nitrogen by
697 marine, planktonic copepods and implications to the marine nitrogen cycle, J. Plankton Res., 7, 553–
698 568, https://doi.org/https://doi.org/10.1093/plankt/7.4.553, 1985.

699 Closset, I., Cardinal, D., Bray, S. G., Thil, F., Djouraev, I., Rigual-Hernández, A. S., and Trull, T. W.:
700 Seasonal variations, origin, and fate of settling diatoms in the Southern Ocean tracked by silicon
701 isotope records in deep sediment traps, Global Biogeochem. Cycles, 29, 1495–1510,
702 https://doi.org/10.1002/2015GB005180, 2015.

703 Demarest, M. S., Brzezinski, M. A., and Beucher, C. P.: Fractionation of silicon isotopes during
704 biogenic silica dissolution, Geochim. Cosmochim. Acta, 73, 5572–5583,
705 https://doi.org/10.1016/j.gca.2009.06.019, 2009.

https://doi.org/10.5194/bg-2022-246
Preprint. Discussion started: 4 January 2023

706 DeVries, T.: Atmospheric CO2 and Sea Surface Temperature Variability Cannot Explain Recent
707 Decadal Variability of the Ocean CO2 Sink, Geophys. Res. Lett., 49, 1–17,
708 https://doi.org/10.1029/2021GL096018, 2022.

709 Egan, K. E., Rickaby, R. E. M., Leng, M. J., Hendry, K. R., Hermoso, M., Sloane, H. J., Bostock, H., and
710 Halliday, A. N.: Diatom silicon isotopes as a proxy for silicic acid utilisation: A Southern Ocean core
711 top calibration, Geochim. Cosmochim. Acta, 96, 174–192,
712 https://doi.org/10.1016/j.gca.2012.08.002, 2012.

713 Ellwood, M. J., Strzepek, R. F., Strutton, P. G., Trull, T. W., Fourquez, M., and Boyd, P. W.: Distinct
714 iron cycling in a Southern Ocean eddy, Nat. Commun., 11, 1–8, https://doi.org/10.1038/s41467-020-
715 14464-0, 2020.

716 Fischer, G., Gersonde, R., and Wefer, G.: Organic carbon, biogenic silica and diatom fluxes in the
717 marginal winter sea-ice zone and in the Polar Front Region: Interannual variations and differences in
718 composition, Deep. Res. Part II Top. Stud. Oceanogr., 49, 1721–1745,
719 https://doi.org/10.1016/S0967-0645(02)00009-7, 2002.

720 Friedrich, J. and Rutgers van der Loeff, M. M.: A two-tracer (210Po-234Th) approach to distinguish
721 organic carbon and biogenic silica export flux in the Antarctic Circumpolar Current, Deep. Res. Part I
722 Oceanogr. Res. Pap., 49, 101–120, https://doi.org/10.1016/S0967-0637(01)00045-0, 2002.

723 Georg, R. B., Reynolds, B. C., Frank, M., and Halliday, A. N.: New sample preparation techniques for
724 the determination of Si isotopic compositions using MC-ICPMS, Chem. Geol., 235, 95–104,
725 https://doi.org/10.1016/j.chemgeo.2006.06.006, 2006.

726 Gleiber, M. R., Steinberg, D. K., and Ducklow, H. W.: Time series of vertical flux of zooplankton fecal
727 pellets on the continental shelf of the western Antarctic Peninsula, Mar. Ecol. Prog. Ser., 471, 23–36,
728 https://doi.org/10.3354/meps10021, 2012.

729 Glibert, P. M., Wilkerson, F. P., Dugdale, R. C., Raven, J. A., Dupont, C. L., Leavitt, P. R., Parker, A. E.,
730 Burkholder, J. M., and Kana, T. M.: Pluses and minuses of ammonium and nitrate uptake and
731 assimilation by phytoplankton and implications for productivity and community composition, with
732 emphasis on nitrogen-enriched conditions, Limnol. Oceanogr., 61, 165–197,
733 https://doi.org/10.1002/lno.10203, 2016.

734 González, H. E., Daneri, G., Iriarte, J. L., Yannicelli, B., Menschel, E., Barría, C., Pantoja, S., and
735 Lizárraga, L.: Carbon fluxes within the epipelagic zone of the Humboldt Current System off Chile: The
736 significance of euphausiids and diatoms as key functional groups for the biological pump, Prog.
737 Oceanogr., 83, 217–227, https://doi.org/10.1016/j.pocean.2009.07.036, 2009.

738 Grasse, P., Brzezinski, M. A., Cardinal, D., De Souza, G. F., Andersson, P., Closset, I., Cao, Z., Dai, M.,
739 Ehlert, C., Estrade, N., François, R., Frank, M., Jiang, G., Jones, J. L., Kooijman, E., Liu, Q., Lu, D.,
740 Pahnke, K., Ponzevera, E., Schmitt, M., Sun, X., Sutton, J. N., Thil, F., Weis, D., Wetzel, F., Zhang, A.,
741 Zhang, J., and Zhang, Z.: GEOTRACES inter-calibration of the stable silicon isotope composition of
742 dissolved silicic acid in seawater, J. Anal. At. Spectrom., 32, 562–578,
743 https://doi.org/10.1039/c6ja00302h, 2017.

744 Grossart, H. P., Kiørboe, T., Tang, K., and Ploug, H.: Bacterial colonization of particles: Growth and
745 interactions, Appl. Environ. Microbiol., 69, 3500–3509, https://doi.org/10.1128/AEM.69.6.3500-
746 3509.2003, 2003.

747 Hansman, R. L. and Sessions, A. L.: Measuring the in situ carbon isotopic composition of distinct
748 marine plankton populations sorted by flow cytometry, Limnol. Oceanogr. Methods, 14, 87–99,
749 https://doi.org/10.1002/lom3.10073, 2016.

750 Hasle, G. R. and Syvertsen, E. E.: Chapter 2 – Marine Diatoms, in: Identifying Marine Phytoplankton,
751 edited by: Tomas, C. R., Academic Press, San Diego, 5–385, 1997.

752 Hatton, J. E., Hendry, K. R., Hawkings, J. R., Wadham, J. L., Opfergelt, S., Kohler, T. J., Yde, J. C., Stibal,
753 M., and Žárský, J. D.: Silicon isotopes in Arctic and sub-Arctic glacial meltwaters: The role of
754 subglacial weathering in the silicon cycle, Proc. R. Soc. A Math. Phys. Eng. Sci., 475,
755 https://doi.org/10.1098/rspa.2019.0098, 2019.

756 Hawco, N. J., Barone, B., Church, M. J., Babcock-Adams, L., Repeta, D. J., Wear, E. K., Foreman, R. K.,
757 Björkman, K. M., Bent, S., Van Mooy, B. A. S., Sheyn, U., DeLong, E. F., Acker, M., Kelly, R. L., Nelson,
758 A., Ranieri, J., Clemente, T. M., Karl, D. M., and John, S. G.: Iron Depletion in the Deep Chlorophyll
759 Maximum: Mesoscale Eddies as Natural Iron Fertilization Experiments, Global Biogeochem. Cycles,
760 35, 1–18, https://doi.org/10.1029/2021GB007112, 2021.

761 Hendry, K. R. and Robinson, L. F.: The relationship between silicon isotope fractionation in sponges
762 and silicic acid concentration: Modern and core-top studies of biogenic opal, Geochim. Cosmochim.
763 Acta, 81, 1–12, https://doi.org/10.1016/j.gca.2011.12.010, 2012.

764 Henley, S. F., Annett, A. L., Ganeshram, R. S., Carson, D. S., Weston, K., Crosta, X., Tait, A., Dougans,
765 J., Fallick, A. E., and Clarke, A.: Factors influencing the stable carbon isotopic composition of
766 suspended and sinking organic matter in the coastal Antarctic sea ice environment, Biogeosciences,
767 9, 1137–1157, https://doi.org/10.5194/bg-9-1137-2012, 2012.

768 Hillebrand, H., Dürselen, C. D., Kirschtel, D., Pollingher, U., and Zohary, T.: Biovolume calculation for
769 pelagic and benthic microalgae, J. Phycol., 35, 403–424, https://doi.org/10.1046/j.1529-
770 8817.1999.3520403.x, 1999.

771 Hilton, J., Lishman, J. P., Mackness, S., and Heaney, S. I.: An automated method for the analysis of
772 “particulate” carbon and nitrogen in natural waters, Hydrobiologia, 141, 269–271,
773 https://doi.org/10.1007/BF00014221, 1986.

774 Honjo, S., Francois, R., Manganini, S., Dymond, J., and Collier, R.: Particle fluxes to the interior of the
775 Southern Ocean in the Western Pacific sector along 170°W, Deep. Res. Part II, 47, 3521–3548,
776 https://doi.org/10.1016/S0967-0645(00)00077-1, 2000.

777 Iversen, M. H., Pakhomov, E. A., Hunt, B. P. V, Jagt, H. Van Der, Wolf-gladrow, D., and Klaas, C.:
778 Sinkers or floaters? Contribution from salp pellets to the export flux during a large bloom event in
779 the Southern Ocean, Deep Sea Res. Part II Top. Stud. Oceanogr., 138, 116–125,
780 https://doi.org/10.1016/j.dsr2.2016.12.004, 2017.

781 Kiørboe, T., Tang, K., Grossart, H. P., and Ploug, H.: Dynamics of microbial communities on marine
782 snow aggregates: Colonization, growth, detachment, and grazing mortality of attached bacteria,
783 Appl. Environ. Microbiol., 69, 3036–3047, https://doi.org/10.1128/AEM.69.6.3036-3047.2003, 2003.

784 Korb, R. E., Whitehouse, M. J., Atkinson, A., and Thorpe, S.: Magnitude and maintenance of the
785 phytoplankton bloom at South Georgia: a naturally iron-replete environment, Mar. Ecol. Prog. Ser.,
786 368, 75–91, https://doi.org/10.3354/meps07525, 2008.

787 Korb, R. E., Whitehouse, M. J., Ward, P., Gordon, M., Venables, H. J., and Poulton, A. J.: Regional and
788 seasonal differences in microplankton biomass, productivity, and structure across the Scotia Sea:
789 Implications for the export of biogenic carbon, Deep Sea Res. Part II Top. Stud. Oceanogr., 59–60,
790 67–77, https://doi.org/10.1016/j.dsr2.2011.06.006, 2012.

791 De La Rocha, C. L., Brzezinski, M. A., and DeNiro, M. J.: Fractionation of silicon isotopes by marine
792 diatoms during biogenic silica formation, Geochim. Cosmochim. Acta, 61, 5051–5056,
793 https://doi.org/10.1016/S0016-7037(97)00300-1, 1997.

https://doi.org/10.5194/bg-2022-246
Preprint. Discussion started: 4 January 2023

794 Manno, C., Stowasser, G., Enderlein, P., Fielding, S., and Tarling, G. A.: The contribution of
795 zooplankton faecal pellets to deep-carbon transport in the Scotia Sea (Southern Ocean),
796 Biogeosciences, 12, 1955–1965, https://doi.org/10.5194/bg-12-1955-2015, 2015.

797 Manno, C., Fielding, S., Stowasser, G., Murphy, E. J., and Thorpe, S. E.: Continuous moulting by
798 Antarctic krill drives major, Nat. Commun., https://doi.org/10.1038/s41467-020-19956-7, 2020.

799 Matano, R. P., Combes, V., Young, E. F., and Meredith, M. P.: Modeling the Impact of Ocean
800 Circulation on Chlorophyll Blooms Around South Georgia, Southern Ocean, J. Geophys. Res. Ocean.,
801 125, 1–18, https://doi.org/10.1029/2020JC016391, 2020.

802 Medlin, L. K. and Priddle, J.: Polar marine diatoms, British Antarctic Survey, Cambridge, UK, 214 pp.,
803 1990.

804 Meyerink, S. W., Boyd, P. W., Maher, W. A., Milne, A., Strzepek, R., and Ellwood, M. J.: Putting the
805 silicon cycle in a bag: Field and mesocosm observations of silicon isotope fractionation in subtropical
806 waters east of New Zealand, Mar. Chem., 213, 1–12,
807 https://doi.org/10.1016/j.marchem.2019.04.008, 2019.

808 Michener, R. and Lajtha, K.: Stable Isotopes in Ecology and Environmental Science: Second Edition,
809 1–566 pp., https://doi.org/10.1002/9780470691854, 2008.

810 Minagawa, M. and Wada, E.: Stepwise enrichment of 15N along food chains: Further evidence and
811 the relation between δ15N and animal age, Geochim. Cosmochim. Acta, 48, 1135–1140,
812 https://doi.org/10.1016/0016-7037(84)90204-7, 1984.

813 Mincks, S. L., Smith, C. R., Jeffreys, R. M., and Sumida, P. Y. G.: Trophic structure on the West
814 Antarctic Peninsula shelf: Detritivory and benthic inertia revealed by δ13C and δ15N analysis, Deep.
815 Res. Part II Top. Stud. Oceanogr., 55, 2502–2514, https://doi.org/10.1016/j.dsr2.2008.06.009, 2008.

816 Montoya, J. P.: Natural abundance of 15N in marine planktonic ecosystems, in: Stable Isotopes in
817 Ecology and Environmental Science: Second Edition, edited by: Michener, R. and Lajtha, K., Blackwell
818 Publishing, 1–566, https://doi.org/10.1002/9780470691854, 2007.

819 Moore, J. K., Abbott, M. R., and Richman, J. G.: Location and dynamics of the Antarctic Polar Front
820 from satellite sea surface temperature data, J. Geophys. Res. Ocean., 104, 3059–3073,
821 https://doi.org/10.1029/1998JC900032, 1999.

822 Ng, H. C., Cassarino, L., Pickering, R. A., Woodward, E. M. S., Hammond, S. J., and Hendry, K. R.:
823 Sediment efflux of silicon on the Greenland margin and implications for the marine silicon cycle,
824 Earth Planet. Sci. Lett., 529, 115877, https://doi.org/10.1016/j.epsl.2019.115877, 2020.

825 Nielsdóttir, M. C., Bibby, T. S., Moore, C. M., Hinz, D. J., Sanders, R., Whitehouse, M., Korb, R., and
826 Achterberg, E. P.: Seasonal and spatial dynamics of iron availability in the Scotia Sea, Mar. Chem.,
827 130–131, 62–72, https://doi.org/10.1016/j.marchem.2011.12.004, 2012.

828 Orsi, H., Whitworth III, T., and Nowlin Jr, W. D.: On the meridional extent and fronts of the Antarctic
829 Circumpolar Current, Deep Sea Res. Part I Oceanogr. Res. Pap., 42, 641–673,
830 https://doi.org/10.1016/0967-0637(95)00021-W, 1995.

831 Passow, U. and De La Rocha, C. L.: Accumulation of mineral ballast on organic aggregates, Global
832 Biogeochem. Cycles, 20, 1–7, https://doi.org/10.1029/2005GB002579, 2006.

833 Pauli, N.-C., Flintrop, C. M., Konrad, C., Pakhomov, E. A., Swoboda, S., Koch, F., Wang, X.-L., Zhang, J.-
834 C., Brierley, A. S., Bernasconi, M., Meyer, B., and Iversen, M. H.: Krill and salp faecal pellets
835 contribute equally to the carbon flux at the Antarctic Peninsula, Nat. Commun., 12, 7168,
836 https://doi.org/10.1038/s41467-021-27436-9, 2021.

https://doi.org/10.5194/bg-2022-246
Preprint. Discussion started: 4 January 2023

837 Popp, B. N., Laws, E. A., Bidigare, R. R., Dore, J. E., Hanson, K. L., and Wakeham, S. G.: Effect of
838 phytoplankton cell geometry on carbon isotopic fractionation, Geochim. Cosmochim. Acta, 62, 69–
839 77, https://doi.org/10.1016/S0016-7037(97)00333-5, 1998.

840 Popp, B. N., Trull, T., Kenig, F., Wakeham, S. G., Rust, T. M., Tilbrook, B., Griffiths, F. B., Wright, S. W.,
841 Marchant, H. J., Bidigare, R. R., and Laws, E. A.: Controls on the carbon isotopic composition of
842 Southern Ocean phytoplankton, Global Biogeochem. Cycles, 13, 827–843,
843 https://doi.org/10.1029/1999GB900041, 1999.

844 Priddle, J. and Fryxell, G.: Handbook of the common plankton diatoms of the Southern Ocean:
845 Centrales except the genus Thalassiosira, British Antarctic Survey, Cambridge, UK, 159 pp., 1985.

846 Rau, G. H., Froelich, P. N., Takahashi, T., and J., D. M. D.: Does sedimentary organic δ13C record
847 variations in quaternary ocean [CO2(aq)], Paleoceanography, 6, 335–347, 1991.

848 Raven, J. A.: Inorganic Carbon Acquisition by Marine Autotrophs, Adv. Bot. Res., 27, 85–209,
849 https://doi.org/10.1016/S0065-2296(08)60281-5, 1997.

850 Rembauville, M., Blain, S., Armand, L., Quéguiner, B., and Salter, I.: Export fluxes in a naturally iron-
851 fertilized area of the Southern Ocean – Part 2: Importance of diatom resting spores and faecal
852 pellets for export, Biogeosciences, 12, 3171–3195, https://doi.org/10.5194/bg-12-3171-2015, 2015.

853 Rembauville, M., Manno, C., Tarling, G. A., Blain, S., and Salter, I.: Strong contribution of diatom
854 resting spores to deep-sea carbon transfer in naturally iron-fertilized waters downstream of South
855 Georgia, Deep. Res. Part I, 115, 22–35, https://doi.org/10.1016/j.dsr.2016.05.002, 2016.

856 Reynolds, B. C., Aggarwal, J., André, L., Baxter, D., Beucher, C., Brzezinski, M. A., Engström, E., Georg,
857 R. B., Land, M., Leng, M. J., Opfergelt, S., Rodushkin, I., Sloane, H. J., Van Den Boorn, S. H. J. M.,
858 Vroon, P. Z., and Cardinal, D.: An inter-laboratory comparison of Si isotope reference materials, J.
859 Anal. At. Spectrom., 22, 561–568, https://doi.org/10.1039/b616755a, 2007.

860 Roberts, K., Granum, E., Leegood, R. C., and Raven, J. A.: Carbon acquisition by diatoms, Photosynth.
861 Res., 93, 79–88, https://doi.org/10.1007/s11120-007-9172-2, 2007.

862 Roca-Marti, M., Puigcorbé, V., Iversen, M. H., Rutgers van der Loeff, M., Klaas, C., Cheah, W.,
863 Bracher, A., and Masqué, P.: High particulate organic carbon export during the decline of a vast
864 diatom bloom in the Atlantic sector of the Southern Ocean, Deep Sea Res. Part II Top. Stud.
865 Oceanogr., 138, 102–115, https://doi.org/10.1016/j.dsr2.2015.12.007, 2017.

866 Salter, I., Kemp, A. E. S. S., Moore, C. M., Lampitt, R. S., Wolff, G. A., and Holtvoeth, J.: Diatom resting
867 spore ecology drives enhanced carbon export from a naturally iron-fertilized bloom in the Southern
868 Ocean, Global Biogeochem. Cycles, 26, 1–17, https://doi.org/10.1029/2010GB003977, 2012.

869 Sathyendranath, S., Brewin, R., Brockmann, C., Brotas, V., Calton, B., Chuprin, A., Cipollini, P., Couto,
870 A., Dingle, J., Doerffer, R., Donlon, C., Dowell, M., Farman, A., Grant, M., Groom, S., Horseman, A.,
871 Jackson, T., Krasemann, H., Lavender, S., Martinez-Vicente, V., Mazeran, C., Mélin, F., Moore, T.,
872 Müller, D., Regner, P., Roy, S., Steele, C., Steinmetz, F., Swinton, J., Taberner, M., Thompson, A.,
873 Valente, A., Zühlke, M., Brando, V., Feng, H., Feldman, G., Franz, B., Frouin, R., Gould, R., Hooker, S.,
874 Kahru, M., Kratzer, S., Mitchell, B., Muller-Karger, F., Sosik, H., Voss, K., Werdell, J., and Platt, T.: An
875 Ocean-Colour Time Series for Use in Climate Studies: The Experience of the Ocean-Colour Climate
876 Change Initiative (OC-CCI), Sensors, 19, 4285, https://doi.org/10.3390/s19194285, 2019.

877 Sathyendranath, S., Jackson, T., Brockmann, C., Brotas, V., Calton, B., Chuprin, A., Clements, O.,
878 Cipollini, P., Danne, O., Dingle, J., Donlon, C., Grant, M., Groom, S., Krasemann, H., Lavender, S.,
879 Mazeran, C., Mélin, F., Müller, D., Steinmetz, F., Valente, A., Zühlke, M., Feldman, G., Franz, B.,
880 Frouin, R., Werdell, J., and Platt, T.: ESA Ocean Colour Climate Change Initiative (Ocean_Colour_cci):

881 Version 5.0 Data, NERC EDS Cent. Environ. Data Anal.,
882 https://doi.org/10.5285/1dbe7a109c0244aaad713e078fd3059a, 2021.

883 Schmidt, K., Atkinson, A., Stübing, D., McClelland, J. W., Montoya, J. P., and Voss, M.: Trophic
884 relationships among Southern Ocean copepods and krill: Some uses and limitations of a stable
885 isotope approach, Limnol. Oceanogr., 48, 277–289, https://doi.org/10.4319/lo.2003.48.1.0277,
886 2003.

887 Scott, F. J. and Marchant, H. J. (Eds.): Antarctic Marine Protists, Australian Biological Resources
888 Study, Canberra, 2005.

889 Shen, C., Dupont, C. L., and Hopkinson, B. M.: The diversity of CO2-concentrating mechanisms in
890 marine diatoms as inferred from their genetic content, J. Exp. Bot., 68, 3937–3948,
891 https://doi.org/10.1093/jxb/erx163, 2017.

892 Sigman, D. M. and Fripiat, F.: Nitrogen isotopes in the ocean, Encycl. Ocean Sci., 263–278,
893 https://doi.org/10.1016/B978-0-12-409548-9.11605-7, 2019.

894 Smetacek, V., Assmy, P., and Henjes, J.: The role of grazing in structuring Southern Ocean pelagic
895 ecosystems and biogeochemical cycles, Antarct. Sci., 16, 541–558,
896 https://doi.org/10.1017/S0954102004002317, 2004.

897 Strickland, J. and Parsons, T.: A Practical Handbook of Seawater Analysis, Fisheries Research Board of
898 Canada, 405 pp., https://doi.org/10.2307/1979241, 1972.

899 Sutton, J. N., Varela, D. E., Brzezinski, M. A., and Beucher, C. P.: Species-dependent silicon isotope
900 fractionation by marine diatoms, Geochim. Cosmochim. Acta, 104, 300–309,
901 https://doi.org/10.1016/j.gca.2012.10.057, 2013.

902 Tamelander, T., Søreide, J. E., Hop, H., and Carroll, M. L.: Fractionation of stable isotopes in the Arctic
903 marine copepod Calanus glacialis: Effects on the isotopic composition of marine particulate organic
904 matter, J. Exp. Mar. Bio. Ecol., 333, 231–240, https://doi.org/10.1016/j.jembe.2006.01.001, 2006.

905 Thorpe, S. E., Heywood, K. J., Brandon, M. A., and Stevens, D. P.: Variability of the southern Antarctic
906 Circumpolar Current front north of South Georgia, J. Mar. Syst., 37, 87–105,
907 https://doi.org/10.1016/S0924-7963(02)00197-5, 2002.

908 Torres Valdés, S., Painter, S. C., Martin, A. P., Sanders, R., and Felden, J.: Data compilation of fluxes
909 of sedimenting material from sediment traps in the Atlantic ocean, Earth Syst. Sci. Data, 6, 123–145,
910 https://doi.org/10.5194/essd-6-123-2014, 2014.

911 Trimborn, S., Wolf-Gladrow, D., Richter, K. U., and Rost, B.: The effect of pCO2 on carbon acquisition
912 and intracellular assimilation in four marine diatoms, J. Exp. Mar. Bio. Ecol., 376, 26–36,
913 https://doi.org/10.1016/j.jembe.2009.05.017, 2009.

914 Trull, T. W. and Armand, L.: Insights into Southern Ocean carbon export from the δ13c of particles
915 and dissolved inorganic carbon during the SOIREE iron release experiment, Deep. Res. Part II Top.
916 Stud. Oceanogr., 48, 2655–2680, https://doi.org/10.1016/S0967-0645(01)00013-3, 2001.

917 Tuerena, R. E., Ganeshram, R. S., Humphreys, M. P., Browning, T. J., Bouman, H., and Piotrowski, A.
918 P.: Isotopic fractionation of carbon during uptake by phytoplankton across the South Atlantic
919 subtropical convergence, Biogeosciences, 16, 3621–3635, https://doi.org/10.5194/bg-16-3621-2019,
920 2019.

921 Volk, T. and Hoffert, M. I.: Ocean Carbon Pumps: Analysis of relative strengths and efficiencies in
922 ocean driven atmospheric CO_2 changes, in: The carbon cycle and atmospheric CO2:Natural variations
923 Archean to Present, edited by: Sundquist, E. T. and Broecker, W. S., American Geophysical Union,

https://doi.org/10.5194/bg-2022-246
Preprint. Discussion started: 4 January 2023

924 Washington, DC, 99–110, 1985.

925 Wada, E. and Hattori, A.: Nitrogen isotope effects in the assimilation of inorganic nitrogenous
926 compounds by marine diatoms, Geomicrobiol. J., 1, 85–101,
927 https://doi.org/10.1080/01490457809377725, 1978.

928 Wada, E., Terazaki, M., Kabaya, Y., and Nemoto, T.: 15N and 13C abundances in the Antartic Ocean
929 with emphasis on the biogeochemical structure of the food web, Deep Sea Res. Part A, Oceanogr.
930 Res. Pap., 34, 829–841, https://doi.org/10.1016/0198-0149(87)90039-2, 1987.

931 Ward, J. P. J., Hendry, K. R., Arndt, S., Faust, J. C., Freitas, F. S., Henley, S. F., Krause, J. W., März, C.,
932 Ng, H. C., Pickering, R. A., and Tessin, A. C.: Stable silicon isotopes uncover a mineralogical control on
933 the benthic silicon cycle in the Arctic Barents Sea, Geochim. Cosmochim. Acta, 329, 206–230,
934 https://doi.org/10.1016/j.gca.2022.05.005, 2022.

935 Weir, I., Fawcett, S., Smith, S., Walker, D., Bornman, T., and Fietz, S.: Winter biogenic silica and
936 diatom distributions in the Indian sector of the Southern Ocean, Deep. Res. Part I Oceanogr. Res.
937 Pap., 166, 103421, https://doi.org/10.1016/j.dsr.2020.103421, 2020.

938 Wetzel, F., de Souza, G. F., and Reynolds, B. C.: What controls silicon isotope fractionation during
939 dissolution of diatom opal?, Geochim. Cosmochim. Acta, 131, 128–137,
940 https://doi.org/10.1016/j.gca.2014.01.028, 2014.

941 White, W. M., Albarède, F., and Télouk, P.: High-precision analysis of Pb isotope ratios by multi-
942 collector ICP-MS, Chem. Geol., 167, 257–270, https://doi.org/10.1016/S0009-2541(99)00182-5,
943 2000.

944 Whitehouse, M. J., Priddle, J., Trathan, P. N., and Brandon, M. A.: Substantial open-ocean
945 phytoplankton blooms to the north of South Georgia, South Atlantic, during summer 1994, Mar.
946 Ecol. Prog. Ser., 140, 187–197, https://doi.org/10.3354/meps140187, 1996.

947 Young, J. N., Heureux, A. M. C., Sharwood, R. E., Rickaby, R. E. M., Morel, F. M. M., and Whitney, S.
948 M.: Large variation in the Rubisco kinetics of diatoms reveals diversity among their carbon-
949 concentrating mechanisms, J. Exp. Bot., 67, 3445–3456, https://doi.org/10.1093/jxb/erw163, 2016.

950